CHAPTER 4 MORE DETAIL ABOUT THE SCANNING IMPEDANCE PROBE

4.1 Summary

This chapter is intended primarily for future users of the high throughput approach described in the previous chapters; other readers may wish to skip to Chapter 5. Section 4.2 describes the parallel characterization approach in more detail. Section 4.3 describes the pulsed laser deposition system used to fabricate graded samples in this work. Section 4.4 gives specifications for the scanning impedance probe. Section 4.5 describes some obstacles to obtaining high quality data and how to overcome them.

4.2 Parallel characterization

A schematic of the typical test configuration in the scanning impedance probe is shown in Figure 4.1. Many features are similar to existing instruments for probing microelectrodes.[9] The typical sample consists of a dense solid $Y_xZr_{1-x}O_{2-x/2}$ (YSZ) electrolyte with an array of thin film microelectrodes patterned on the top face. A porous counter electrode is applied over the entire bottom face. The sample is placed on a stage heater with a thin piece of ceramic insulation to provide electrical insulation between the sample and the stage. A metal wire is used to connect the counter electrode to the negative terminal of an external impedance analyzer. The chamber is sealed, and the sample is heated to high temperature while the desired test gas flows continuously through the chamber. A metal probe

tip is touched to an individual microelectrode in order to make an electrical connection to the positive terminal of the impedance analyzer, and an impedance spectrum (or d.c. voltammogram) can then be acquired. The probe tip is moved or the conditions are adjusted, another impedance spectrum is acquired, and so on until the study is completed. An external optical microscope peers through a quartz viewport in the chamber ceiling, enabling the user to view the position of the metal probe tip relative to the micropatterned features on the sample.

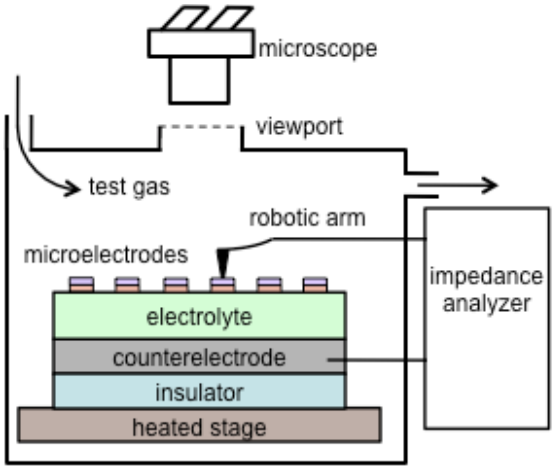

Figure 4.1. Schematic of the test configuration in the scanning impedance probe.

The most significant new feature of the scanning impedance probe is the "scanning" capability: the position of the alumina rod holding the metal probe tip is controlled by three orthogonal lead screws controlled by stepper motors. Thus the metal probe tip can be touched to a microelectrode simply by entering the appropriate (X,Y,Z) coordinates in the control software developed by the author. By extension, hundreds of microelectrodes can be contacted and measured in

sequence simply by listing their coordinates. The control software also allows for automated control of stage temperature, gas flows, and other settings such as wait times between steps, d.c. bias voltage, a.c. perturbation voltage, and so on. Since a single impedance spectrum typically takes 1 min - 15 min to acquire, depending on the chosen frequency range, the scanning impedance probe can measure between 100 and 1500 spectra per day. So for instance, at 5 min per spectrum, a study of 100 microelectrode compositions at five gas pressures and four temperatures can be completed autonomously in about one week.

Automation also facilities precise vertical positioning of the probe; too high and the tip does not touch the sample at all; too low and the tip is jammed into the sample, which can introduce error in the tip position and damage the tip or the sample. The scanning impedance probe automatically detects the contact by repeatedly measuring the impedance at a single frequency as the tip is slowly lowered.

4.3 Parallel fabrication

Two example layouts for the microelectrode arrays are shown schematically in Figure 4.2. The outer dimensions of these layouts correspond to typical commercially-available substrate sizes of 5 mm x 10 mm (left layout) and 10 mm x 10 mm (right layout). Each circle represents a single microelectrode, and the area between the circles represents exposed substrate. The left layout includes a diameter gradient, while the right layout has a fixed diameter (125 um). In the

horizontal direction of each layout and in the vertical direction of the right layout, another property besides diameter can be graded.

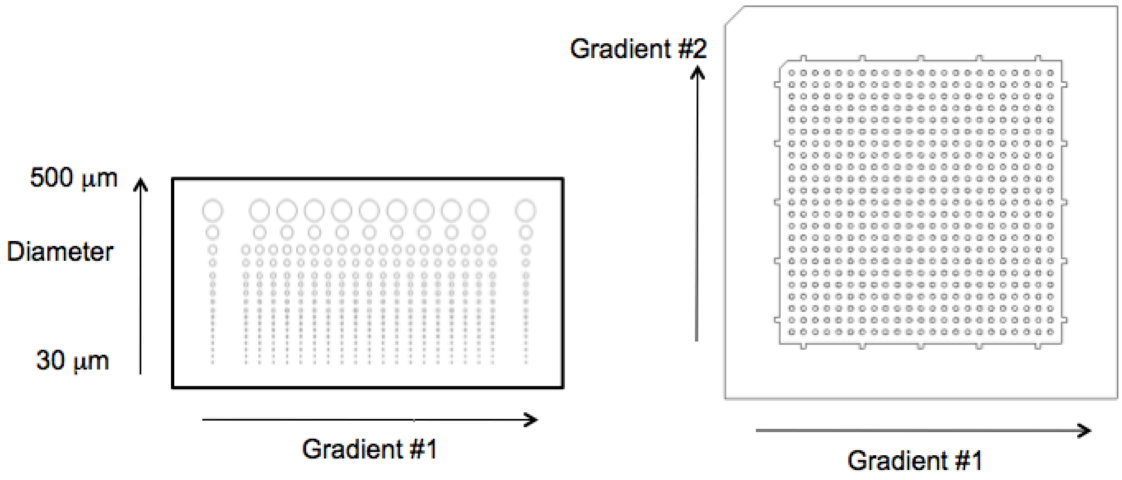

Figure 4.2. Example layouts of microelectrodes on a sample. Left: 17 x 21 = 357 microelectrodes (including 11 different diameters) on a 5 mm x 10 mm substrate. Right: 23 x 23 = 529 microelectrodes on a 10 mm x 10 mm substrate.

Previous microelectrode studies have not reported gradients of properties other than microelectrode diameter/area. Yet many properties can conceivably be graded, as illustrated in Figure 4.3.

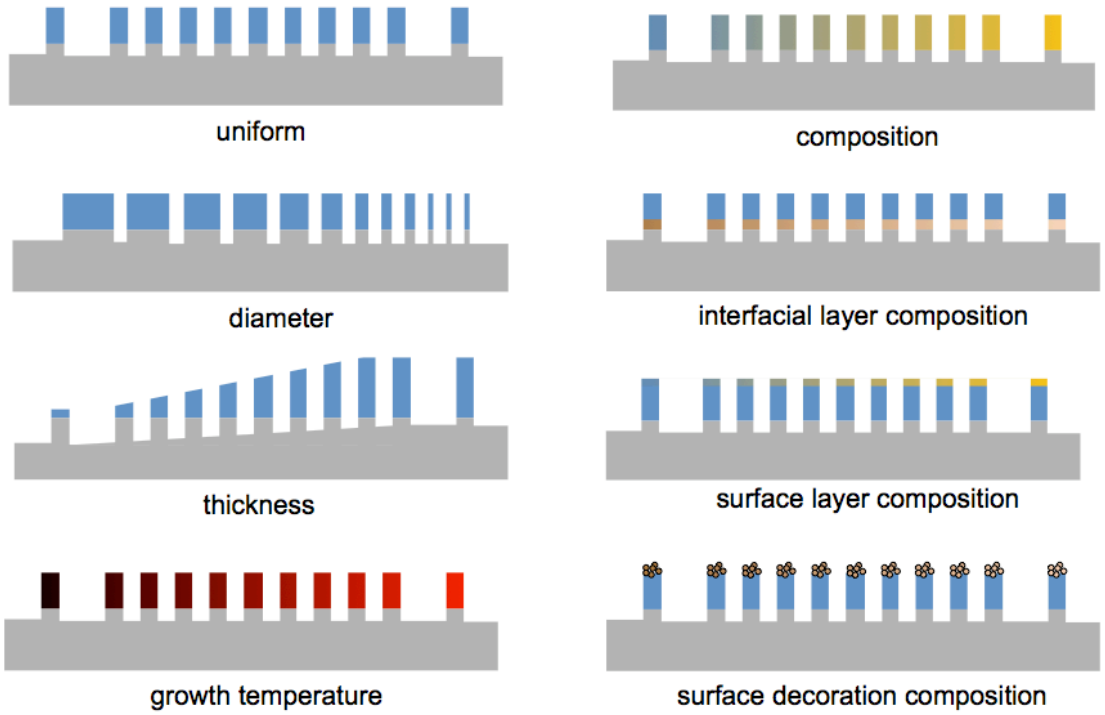

Figure 4.3. Examples of properties that can be systematically varied along the rows and/or columns of a microelectrode array.

This approach of combining graded samples with automated impedance measurement can potentially give insight into a variety of important questions. For example, in the material system $La_{0.5}Sr_{0.5}Co_{1-y}Fe_yO_{3-\delta}$ what level of iron doping results in the highest activity towards oxygen electro-reduction? Do all levels of iron doping provide equal long-term stability? Does film thickness matter, or is there facile ion diffusion through the film? Can strain effects be seen by varying the composition of an interfacial layer? Can the activity be influenced by decorating the catalyst surfaces with trace amounts of another substance? And of course, when interesting trends in activity are identified, the graded samples can be probed by numerous other techniques besides impedance spectroscopy, so that

correlations can be investigated between electrochemical activity and properties like film orientation, grain boundary density, surface electronic structure, and so on.

Fabrication of the arrays shown in Figure 4.3 is possible by many routes. In the work described in the previous chapters, the gradient samples were prepared by Shingo Maruyama (a member of the Professor Ichiro Takeuchi's group at the University of Maryland) using pulsed laser deposition in combination with movable shutters and appropriate stages. This method is described elsewhere[60] and briefly summarized here. Two targets with the end member compositions A and B are used. By frequently altering which target is ablated while drawing a shutter back and forth across the sample, a library with the composition spread A_xB_{1-x} is obtained. At first glance it may appear that the resulting film would have numerous interwoven layers, however the deposition is typically done at high enough temperature that the diffusion length is larger than the layer thickness (~1 monolayer) but far smaller than the sample length (1 cm). Thus in terms of composition, the growth achieves out-of-plane homogeneity while retaining in-plane heterogeneity. Alternatively, by using one target and slowly drawing the shutter across the sample a single time, a thickness gradient is achieved in a single composition. Another option is the use of a stage with asymmetric geometry, as described in the last chapter, that can achieve a lateral temperature gradient of 200˚C - 300˚C between the ends of a 1 cm substrate. An exciting possibility in development is to fabricate not just binary libraries but ternary or quaternary

libraries. For example, with appropriate shutter motions it should be possible to obtain quaternary library shown in Figure 4.4. Similar libraries have been demonstrated for luminescent and magnetic materials.[60] In all cases, after the growth, photolithography and ion milling are used to etch away the undesired portions of the film, leaving behind the microelectrode pattern as shown in Figure 4.2.

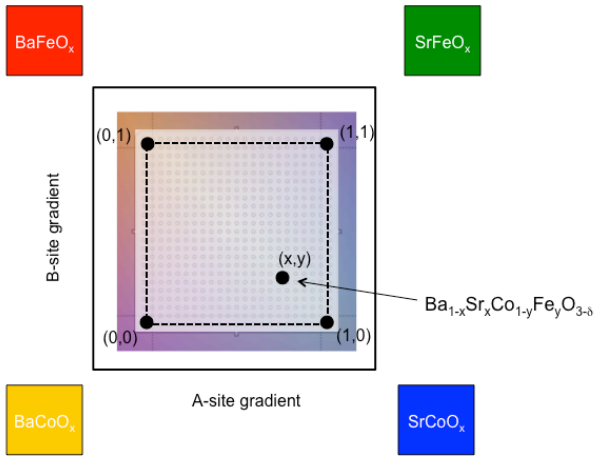

Figure 4.4. Schematic of a quaternary library that could be made from four binary targets ($BaFeO_x$, $SrFeO_x$, $BaCoO_x$, and $SrCoO_x$) to span the family of compositions $Ba_{1-x}Sr_xCo_{1-y}Fe_yO_{3-\delta}$, where x,y ε [0,1].

4.4 Scanning Impedance Probe: Details

4.4.1 Mechanical

Photos of the scanning impedance probe exterior are shown in Figure 4.5 and Figure 4.6. Typical sample installations are shown in Figure 4.7.

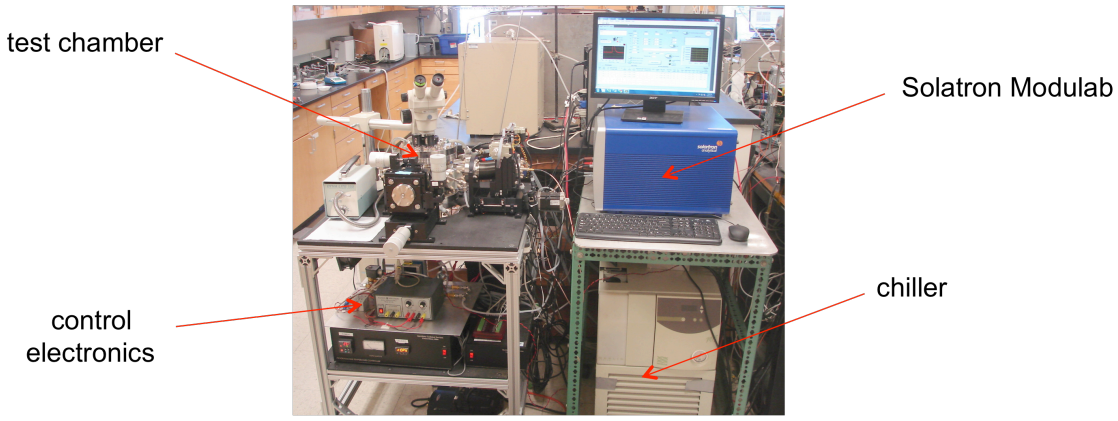

Figure 4.5. Scanning impedance probe system.

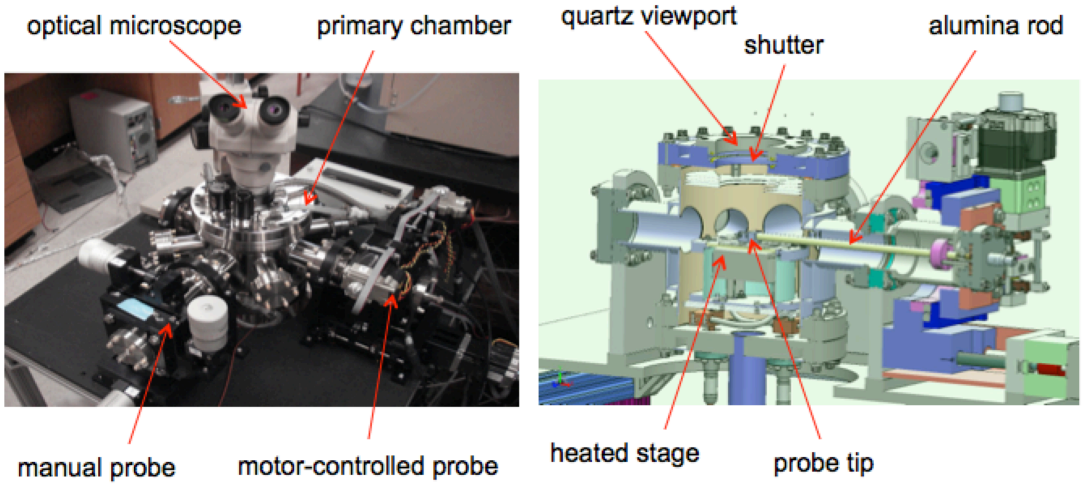

Figure 4.6. Primary chamber of the scanning impedance probe. Left: external photo. Right: computer model cross-section, showing the chamber interior.

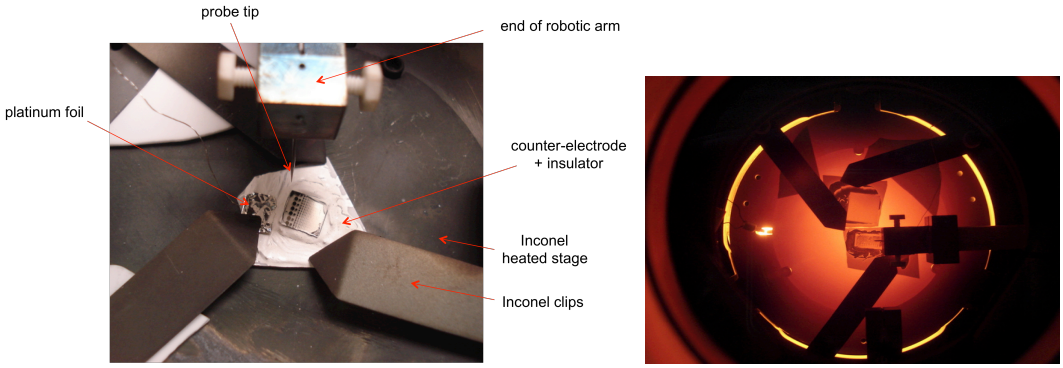

Figure 4.7. Typical sample configurations inside the scanning impedance probe. Left: at room temperature with added illumination. Right: a different sample at ~800˚C sample temperature with no added illumination.

4.4.2 Thermal

The temperature of the Inconel stage is measured by a K-type thermocouple spot-welded to the stage underside, and can be heated well above 1000˚C. In practice, a maximum stage temperature of ~ 800˚C is recommended to avoid sample contamination. Green discoloration of a blank white polycrystalline alumina substrate was observed upon annealing with a stage temperature of 1000˚C. Separately, Mo was detected on LSM/YSZ samples by both EDS and XPS on samples annealed for several days at a stage temperature of 840˚C. No such contamination was observed on samples annealed on a 700˚C stage for several days. The chamber walls, floor, and ceiling are protected from corrosion by chilled water that is circulated through internal channels, so the heating element and Inconel stage components are the likely impurity sources at > 800˚C.

The stage has a diameter of 50 mm, however it is visually evident in Figure 4.7 that only the central region with diameter of ~ 20 mm is heated to a uniform temperature (< 10˚C variation, estimated by probing a representative sample in the stage center with a thermocouple attached to the system's manual probe arm).

At steady state, the stage temperature is maintained constant within ± 1-2˚C of the target value. However, radiative and convective cooling cause the sample surface temperature to be lower than the stage temperature. A calibration run was performed with a 0.5 mm diameter thermocouple silver-pasted to a representative YSZ substrate, as shown in Figure 4.8. The results depended slightly on whether the viewport shutter is open or closed. Equations (1) and (2) are the calibration curves. For instance, for a stage temperature of 750˚C, the sample surface temperature is ~ 720˚C with the shutter closed.

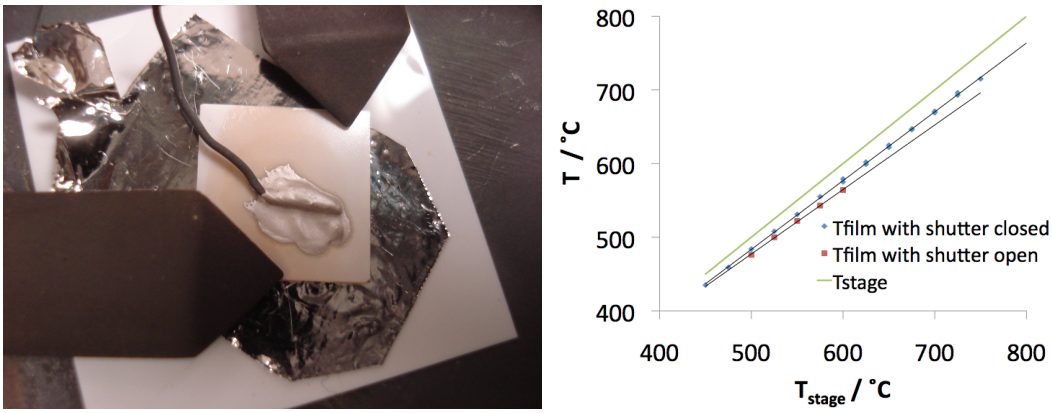

Figure 4.8. Calibration of the sample surface temperature. Left: measurement configuration. Right: Measured "film" temperature plotted vs. the stage (a.k.a. element) temperature.

$$T_{film} = 0.934 T_{stage} + 17 \qquad \text{shutter closed} \qquad (1)$$

$$T_{film} = 0.876 T_{stage} + 39 \qquad \text{shutter open} \qquad (2)$$

4.4.3 Gas Control

The sealed chamber is high vacuum compatible, and leak rates are low enough that using suitable inlet mixtures of nitrogen and oxygen, oxygen partial pressures below 10^{-4} atm can be maintained. All internal chamber components including the $MoSi_2$ heating element can nominally withstand reducing gases like hydrogen or methane. Gas mixing is accomplished with external mass flow controllers. The purge time for changing the chamber gas environment depends on the initial and final gas compositions; for oxygen-nitrogen mixtures with flow rate greater than 100 sccm, using an external oxygen sensor, the longest observed equilibration time was under 3.5 hours (which occurred when switching from 100% O_2 to 0.01% O_2). Typical purge times are under one hour. Studies under low humidity are possible if

the inlet gas is pre-humidified, and studies under high humidity may be possible if the water circulated through the chamber walls is heated instead of chilled.

4.4.4 Electronic

Either a Solartron Modulab or a Solartron 1260 impedance analyzer can be used to acquire impedance measurements. Detailed specifications for the impedance measurement accuracy can be found in the user manuals for those instruments.

4.4.5 Software

The scanning impedance probe system includes a substantial Labview-based software driver, which reads the program sequence (including which microelectrodes should be measured, and under which conditions) from an Excel spreadsheet and logs all measured data to text files.

Note that upon changing the stage temperature, the various chamber components expand and contract by varying amounts, and thus the microelectrode coordinates are different at every temperature. To account for this effect, three reference points are measured at two reference temperatures. Coordinate transformations are then used to calculate all the microelectrode positions at all temperatures, assuming the expansion effect can be linearly interpolated/extrapolated. The positional errors introduced by this assumption are modest.

4.5 Some obstacles to obtaining good data, and how to overcome them

4.5.1 Tip Cooling

The metal probe is cooler than the sample, so the probe tip has the effect of locally cooling the sample by conduction during each impedance measurement. For large enough electrodes, this local cooling can be neglected. However, as the electrode diameter decreases, a larger fraction of the electrode area will be affected by the cooling. In other words, the smaller the microelectrode diameter, the more the average electrode temperature is expected to be lowered by tip cooling.

This effect was first mentioned by Opitz and Fleig[35] in 2010; it appears to have been neglected in the many microelectrode papers using solid electrolytes published before 2010. Opitz and Fleig reported Seebeck voltages of tens of millivolts between the sample electrodes as a result of this cooling. A similar but smaller effect was observed in this work. Specifically, thermovoltages in the presence of tip cooling were measured as a function of stage temperature and dot diameter. The results are plotted in Figure 4.9. These results were independent of gas flow rate up to the max flow rate attempted (300 sccm). Next, the thermovoltage was measured on a relatively large area electrode (0.5 cm^2) to assess the temperature drop across the sample when tip cooling is negligible. The large area makes the impact of tip cooling negligible. This Seebeck voltage can thus be attributed to convection/radiation losses only, and is shown for different temperatures as horizontal lines in Figure 4.9.

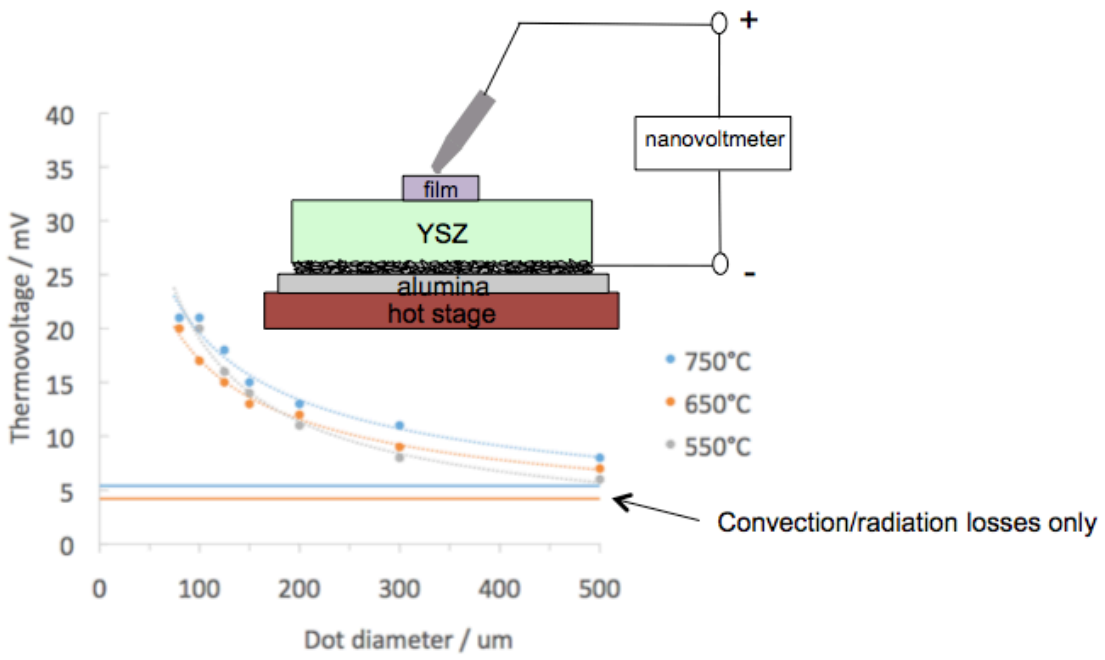

Figure 4.9. Measured voltage drop V_{film} - $V_{counter\ electrode}$ across the YSZ substrate using an $La_{0.5}Sr_{0.5}CoO_{3-d}$ microelectrode and a tip made of Paliney7 (a noble metal alloy containing primarily palladium).

The precise amount of tip cooling varies between measurements depending on the thermal conductivities of the sample and tip and the thermal resistance at the tip contact. Also, the temperature profile did not always instantly reach steady state; it typically took 5 s - 180 s for the thermovoltage to stabilize, with the faster times corresponding to higher temperatures or larger diameters. To correct for tip cooling, the scanning impedance probe waits for a user-specified time after contacting the sample, measures the thermovoltage, and then proceeds with the impedance measurement. The temperature drop across the sample can then be estimated from the measured thermovoltage if the substrate Seebeck coefficient is known. For example, the Seebeck coefficient of YSZ is ~ 0.5 mV/K.[36]

The ability to measure the thermovoltage immediately prior to acquiring each impedance spectrum had not yet been implemented when the data in this thesis were taken, so all reported film temperatures are corrected based on the set of thermovoltages reported in Figure 4.9. The error introduced by this approximated correction is not expected to be severe.

4.5.2 Tip scratching

Some tips easily scratch some films. The extent of scratching depends on the tip hardness, film hardness, and the contact force, which in turn depends on the geometry and stiffness of the probe. In this work it was found that Paliney7 probes (20 mm - 35 mm length, 0.5 mm shank diameter, 40 μm tip diameter) are able to repeatedly probe both oxide and metal films with negligible scratching. Paliney7 is a palladium-based noble metal alloy that exhibits good oxidation resistance, and probe tips made of Paliney7 are sold commercially for probing applications at high temperatures.

Literature reports of microelectrode measurements typically use PtIr or Pt-plated tungsten, however the former were found to frequently scratch both metal films (*e.g.*, Pt) and oxide films (*e.g.*, LaSrMnO3), while with the latter, the plating appeared to scrape off over time, leading to tungsten oxide growth and distorted measurements.

4.5.3 Electronic noise and artifacts

The control thermocouple (spot-welded to the underside of the stage) acts as a pathway for electrical noise to enter the chamber, which otherwise acts as a Faraday cage. The impact of this noise can be minimized by: (1) installing samples such that the counter-electrode is electrically insulated from the stage; (2) increasing the applied perturbation voltage; (3) not connecting multiple thermocouples to the stage; and (4) electrically shielding the thermocouple wire exiting the bottom of the chamber.

Temperature fluctuations can also add noise to the measured impedance spectra, and in particular, the chamber heating control is sensitive to fluctuations in electrical voltage in the heater power supply. For example, plugging a small chiller into the same outlet as the heater can cause temperature fluctuations of several degrees that add significant noise to the measured impedance spectra, particularly at low frequencies. It is recommended that the heater power cable be given a power conditioner and a dedicated outlet.

The Solartron Modulab impedance analyzer has software flaws that can cause it to violate its accuracy specifications. First, at high frequencies the Modulab "auto-current-ranging" algorithm typically chooses a suboptimal current range, which leads to spurious inductance that distorts high frequency features, as shown at left in Figure 4.10. At the time of writing, the manufacturer claimed to be working on a solution. In the meantime, a custom auto-ranging algorithm was implemented in

Labview which eliminates this spurious inductance by dividing a single impedance spectrum into several scans at different current ranges. However, a second flaw in the Modulab software makes it impossible to avoid switching to open circuit between scans, which causes spurious "jumps" when the circuit under test has a small capacitance. An example of such a jump is shown at right in Figure 4.10. Also, briefly switching to open circuit between scans has the effect of turning off and on any d.c. bias that is applied, which can introduce artifacts into impedance measurements under d.c. bias. Until the manufacturer produces a revised software driver, bias measurements and measurements on samples with low capacitance should use the Modulab auto-ranging algorithm, with a correction at high frequencies to account for the spurious inductance. For all other measurements, the custom auto-ranging is probably more accurate.

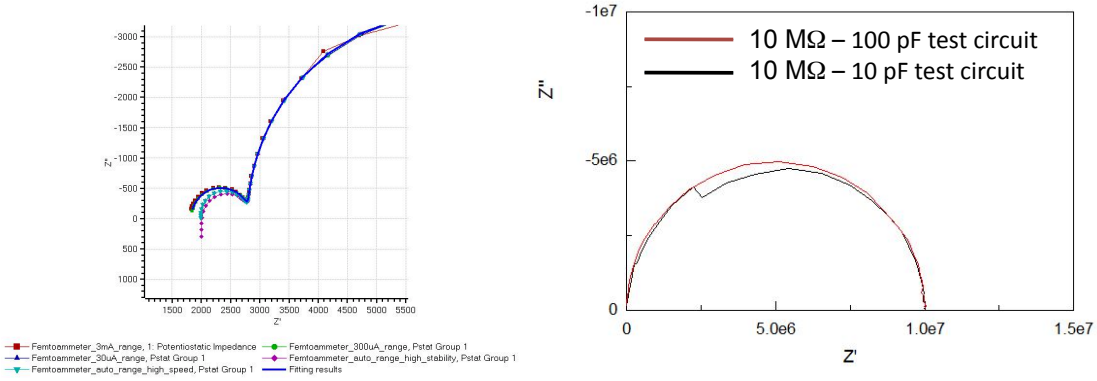

Figure 4.10. Left: Spurious inductance at high frequencies, caused by improper choice of current range. Right: Spurious jump in the data upon changing current ranges for low capacitance samples.

4.5.4 Contamination

Molybdenum contamination has been observed on some films after prolonged testing in the scanning impedance probe at elevated temperatures. Specifically, MoO_3 particles were detected on $LaSrMnO_3$ films by XPS, SEM, and EDS after 130 h testing at T_{stage} = 840˚C. The particles were not observed on the surrounding YSZ substrate. Films tested for a similar time no higher than T_{stage} = 750˚C exhibited no such contamination. The chamber has a $MoSi_2$ heating element and a stage made of Inconel 625 (a nickel superalloy that contains Mo), and these are likely responsible for the contamination. For operation above T_{stage} = 750˚C, blocking gaps to the heating element and switching to a Mo-free stage (*e.g.*, Inconel 600) are recommended.

Silver contamination has also been observed on some films after testing. Specifically, silver particles were detected by XPS, SEM, and EDS after testing up to T_{stage} = 675˚C for samples prepared with a silver paste counter electrode. Evidently silver is quite mobile in oxygen-containing atmospheres, and although the film's bulk properties are likely unaffected, the presence of silver may have an impact on catalytic activity.[51] As such, the use of silver should probably be avoided in most surface studies. Some of the results reported in the next chapter are preliminary in nature and used a silver counter electrode for expediency.

4.5.5 Sheet resistance

Sheet resistance may contribute to the impedance spectra of microelectrodes that are sufficiently thin with sufficiently large diameter and low electronic conductivity. This contribution can distort the impedance spectra at high frequencies, while typically leaving the low frequency fit parameters largely unaffected.[15] In this work, owing to the high electronic conductivity of the film materials studied, sheet resistance made a small contribution to the measured offset resistance and was otherwise negligible.